J Parasit Dis (Jan-Mar 2018) 42(1):102–113
https://doi.org/10.1007/s12639-017-0973-8

ORIGINAL ARTICLE

Assessment of spiramycin-loaded chitosan nanoparticles treatment on acute and chronic toxoplasmosis in mice

Samia E. Etewa[1] · Dalia A. Abo El-Maaty[1] · Rania S. Hamza[1] · Ashraf S. Metwaly[1] · Mohamed H. Sarhan[1] · Sara A. Abdel-Rahman[1] · Ghada M. Fathy[1] · Mahmoud A. El-Shafey[2]

Received: 30 October 2017 / Accepted: 6 December 2017 / Published online: 15 December 2017

Abstract Toxoplasmosis is a zoonotic parasitic disease with worldwide distribution. Chitosan is a natural polymer which is commonly used in the production of nanomedicines. It is known to enable higher drug permeation, being biocompatible and has very low toxicity, besides its antimicrobial effects. Our study aimed to assess the effect of spiramycin-loaded chitosan nanoparticles (SLCNs) in treatment of acute and chronic toxoplasmosis in mice. 200 male Swiss albino mice were included in our study, divided to two main groups; *Toxoplasma gondii* RH strain infected group and ME49 strain infected group, each main group was subdivided into four subgroups; subgroup I: infected control, subgroup II: infected and received chitosan nanoparticles (CS NPs); 20 µg of CS NPs in 100 µl of PBS/mouse/dose, subgroup III: infected and treated with spiramycin (Rovamycin); 100 mg/kg/day, subgroup IV: infected and treated with 100 mg/kg/day spiramycin-loaded chitosan nanoparticles. Effect of treatment was assessed parasitologically and histopathologically. It was noticed that SLCNs significantly decreased the mortality rate of infected mice with both strains compared to high mortality rate of mice in the infected control subgroups. Moreover, there was a significant decrease in the number of organisms of SLCNs treated subgroup as compared to the other subgroups. Histopathological studies showed a marked improvement of the pathological pictures of brain, liver, spleen and eye in the subgroup received SLCNs as opposed to other groups. In conclusion, the present study revealed that loading of spiramycin on chitosan nanoparticles increased its antiparasitic effect on acute and chronic *T. gondii* infection.

Keywords Toxoplasmosis · spiramycin · Nanoparticles · Treatment · Histopathology

Introduction

Toxoplasmosis is a parasitic disease with global distribution. It is caused by an obligate intracellular coccidian parasite; *Toxoplasma gondii* (*T. gondii*) (El-On and Peiser 2003). Man catches infection by ingesting undercooked meat containing tissue cysts, or from contamination with oocysts in feces of cats. Infection is almost asymptomatic, but severe pathological changes are common in cases of congenital infection and immunodeficiency (Jongert et al. 2009).

Treatment of toxoplasmosis is almost target the tachyzoite which is active, rapidly replicating and disseminates throughout the body causing tissues destruction. Whereas, bradyzoites and tissue cysts aren't affected by treatment as they have less metabolic activity, and they are protected by the blood–brain barrier (Cottrellm 1986; Israelski and Remington 1993).

Spiramycin is produced by *Streptomyces ambofaciens* and contains three 16-membered macrolide antiparasitics and antibiotics (Kernbaum 1985; Rubinstein and Keller 1998). It is used in the treatment of toxoplasmosis (Engel et al. 2000) and cryptosporidiosis (Perng et al. 2003). It is used also in the treatment of different soft tissues infections, such as digestive (Bunetel et al. 2001), respiratory (Bunetel et al. 2001), urinary and reproductive systems

✉ Sara A. Abdel-Rahman
sarameram@yahoo.com

[1] Medical Parasitology Department, Faculty of Medicine, Zagazig University, Zagazig, Egypt

[2] Clinical Pathology Department, Faculty of Medicine, Zagazig University, Zagazig, Egypt

(Mourier and Brun 1997). Spiramycin has minimal foetal toxicity and it prevents the spreading of the parasite to the fetus through the placenta (Montoya and Remington 2008).

The bioavailability of any drug, including spiramycin, is affected by many factors such as membrane permeability and solubility (Mourier and Brun 1997). Studies were done to increase the solubility of the drugs which have poor water-solubility and its dissolution rate (Farinha et al. 2000; Choi et al. 2004; Paradkar et al. 2004).

Drugs which are used in the treatment of toxoplasmosis produce sound effects and can cross biological barriers, with minimal toxic side effects, are not yet available (Briones et al. 2008).

Nanotechnology is the science involves small sized materials with diameters range from tens to hundreds of nanometers. This size can change many physicochemical and biochemical properties of the cells by affecting several biomolecules on the cells surfaces and intracellularly (Salata 2004).

Nanoparticles can act as drug carriers that can modulate pharmacokinetics, increase bioavailability and target release with minimal toxic effects (Khalil et al. 2013).

Polymeric nanoparticles have biocompatibility and biodegradable characteristics, where the therapeutic agent can be dissolved, absorbed, or encapsulated in the polymer matrix. They may contain synthetic polymers (poly (D,L-lactic-co-glycolic acid), polyethylene glycol, or polyester biobeads) and materials from natural sources as alginate, insulin and chitosan (Chan et al. 2010).

Chitosan is a polysaccharide (partially or fully deacetylated chitin), which has been used in the medical field during the last two decades. It is an important material for the nanoparticles preparation as it is biodegradable and nontoxic (Ing et al. 2012). So, it is used as an antibacterial and antifungal product (Kean and Thanou 2010).

Many studies have been done on chitosan nanoparticles (CS NPs) to assess its anti-parasitic effects; they produced mild protection in treatment of *Giardia lamblia* infection (Said et al. 2012), increased the effect of ivermectin as anti-filarial drug (Ali et al. 2013).

Our study aimed to assess the effect of spiramycin-loaded chitosan nanoparticles in treatment of acute and chronic toxoplasmosis infection in mice.

Materials and methods

Strains

Both virulent *T. gondii* (RH strain) and avirulent (ME49 strain) were obtained from Medical Parasitology Department, Faculty of Medicine, Alexandria University and maintained in Medical Parasitology Department, Faculty of Medicine, Zagazig University.

Virulent *T. gondii* strain (RH strain)

Maintenance of RH virulent strain was done by serial intraperitoneal injection of tachyzoites in Swiss albino mice (6–8 weeks old, 20 g weight) every 3–4 days intervals. Tachyzoites were collected after 4 days post infection from the peritoneal exudates and washed three times in phosphate buffer solution (PBS) at pH (7.4). Then, they were diluted with PBS with pH 7.4 and used for infection of mice at a dose of 3.5×10^3 tachyzoites per mouse (Chan and Luft 1986; Saudi et al. 2008).

Avirulent *T. gondii* strain (ME49 strain)

Maintenance of ME49 strain was done by repeated intraperitoneal injection of Swiss albino mice every 8 weeks, with 0.1 ml of brain suspension containing $1x10^2$ cysts per ml of previously infected mice (El-Sayed and Aly 2014).

Mice grouping and experimental design

200 male Swiss albino mice, aged 6–8 weeks and weighed 20–25 g, were included in our study. They were housed in well ventilated cages and fed standard pellet food with free access to water (El-Fakhry et al. 1998). Examination of mice faeces was done to exclude any parasitic infection (Giarcia and Bruckner 1977). They were divided to two main groups; the 1st group (100 mice) was infected by *T. gondii* RH strain, then it was subdivided to four equal subgroups; 25 mice each. Subgroup I: RH strain infected control, subgroup II: infected group taken chitosan nanoparticles (CS NPs); received 20 µg of CS NPs in 100 µl of PBS per mouse per day, subgroup III: infected group treated with spiramycin (Rovamycin); 100 mg/kg/day (Filice and Pomeroy 1991), subgroup IV: infected group treated with 100 mg/kg/day spiramycin-loaded chitosan nanoparticles. Treatment began on the second day of infection daily for 7 days. 5 days post infection, 5 mice out of 25 were sacrificed and the other 20 mice were observed daily to assess the mortality rate. The 2nd group (100 mice); infected by *T. gondii* ME49 strain, then it was subdivided to four equal subgroups; 25 mice each. Subgroup I; ME49 strain infected control group, subgroup II: ME49 strain infected group taken chitosan nanoparticles; received 20 µg of CS NPs in 100 µl of PBS/mouse/day, subgroup III: ME49 strain infected group treated with spiamycin (Rovamycin); received 100 mg/kg/day, subgroup IV: ME49 strain infected group treated with100 mg/kg/day spiramycin-loaded chitosan nanoparticles. After

6 weeks post-infection; mice were treated daily for 10 days. 60 days post infection, 5 mice out of 25 were sacrificed and the other 20 mice were observed daily to assess the mortality rate.

Materials

Chitosan; 93% degree of deacetylation and sodium tripolyphosphate were purchased from Sigma-Aldrich, USA. Phosphate buffer saline (PBS) and acetic acid were purchased from Sigma-Aldrich, USA. Spiramycin (Rovamycin) was obtained from sanofi-aventis, Egypt.

Ionic gelation method for chitosan nanoparticles preparation (CS NPs)

Chitosan nanoparticles were synthesized via the ionotropic gelation of chitosan with Tripolyphosphate (TPP) anions. TPP has been used to prepare (CS NPs) as it is nontoxic, multivalent and has the ability for gels formation via ionic interactions. The charge density of TPP and chitosan can control this interaction, under the influence of the solution pH. Chitosan was dissolved at various concentrations of acetic aqueous solution; 1, 2 and 3 mg/ml. The chitosan concentration was 1.5 times lower than that of acetic acid in aqueous solution. The TPP solution (1 mg/ml) was prepared by double-distilled water. CS NPs were made-up with the drop wise adding of 5 ml of the chitosan solution on 2 ml of TPP solution under 1000 rpm magnetic stirring for 1 h at room temperature. The suspension was performed under the same above-mentioned conditions. Separations of the nanoparticles were done by centrifugation at 20000 g at 14 °C for 30 min, and then they were freeze-dried and stored at 4 °C. Their weights were measured, and they were characterized using scanning electron microscope (SEM) (JEOL 100 CX) (Somnuk et al. 2011).

Spiramycin-loaded chitosan nanoparticles (SLCNs)

SLCNs were made by adding chitosan solution to TPP solution (containing spiramycin at a concentration of 100 mg/ml). SLCNs were separated from the suspension by centrifugation (20000 g at 14 °C) for 30 min. Then, sediment was collected and weighed. The total protein content/mg of chitosan encapsulating powder was calculated by dividing the protein concentration of the loaded spiramycin by the nanoparticles weight (Danesh-Bahreinni et al. 2011). The loading efficiency of the nanoparticles was determined:

$$\%\mathrm{LE} = \frac{\mathrm{A} - \mathrm{B}}{\mathrm{A}} \times 100$$

A: The total protein concentration of spiramycin. B: The concentration of proteins in supernatant.

Evaluation of the treatment efficacy

I. Parasitological study

All the experimental groups were subjected to the following:

1. Estimation of the mortality rate (MR) (Eissa et al. 2012):

$$\mathrm{MR} = \frac{\text{Number of dead mice at the sacrifice time}}{\text{Number of mice at the beginning of the experiment}} \times 100$$

2. Morphological study of *T. gondii* tachyzoites:

At the 5th day post infection, collection of the peritoneal fluid containing tachyzoites was done from all RH strain infected groups separately and examined by light microscopy (LM).

3. Estimation of the parasite count

T. Gondii tachyzoites and bradyzoites were counted in impression smears stained with Giemsa, from different tissues (brain, liver and spleen) of virulent RH infected mice subgroups, and in the brain and the liver of mice subgroups infected with ME49 strain. All studied organs in each mouse were examined using oil immersion and the mean of 10 different fields was calculated and then the mean was calculated for each subgroup (Araujo et al. 1992; Thiptara et al. 2006; Barakat 2007).

The % reductions in the mortality rate and the parasite count were calculated according to the following equation:

$$\%\mathrm{R} = \frac{100(C - E)}{C}$$

%R: % reductions, C: control group and E: experimental groups of mice (Penido et al. 1994).

II. Histopathological evaluation

Specimens from different tissues (brain, liver, spleen and eye) were fixed in formalin (10%) and dehydrated in ascending grades of ethyl alcohol, then they were cleared in xylol, and embedded in paraffin wax. Sections of 5 µm thickness were cut and stained using haematoxylin and eosin (H&E) stain (Drury and Wallington 1980) and Periodic acid-Schiff (PAS) stain (Yamabayashi and Tsukahara 1987).

Ethical consideration

The study was conducted according to the regulations of the Ethics Committee of Zagazig University, based on international regulations of animal care.

Statistical analysis

Data were presented as mean ± SD and median. Data analysis was done using SPSS version 20. ANOVA F-test was used to calculate difference between quantitative variables among subgroups and Mann–Whitney test was used for comparison between two groups (Chan 2003). P value < 0.05 indicates significant results (Leslie et al. 1991).

Results

Nanoparticles characterization

By SEM, spiramycin-loaded chitosan nanoparticles (SLCNs) were regular, rounded and have a smooth surface. Their mean size was 60.08 ± 2.009 nm (Fig. 1a, b).

Parasitological study

- Mortality rate

The least mortality rate among RH infected mice was observed in infected subgroup treated with SLCNs; 75% of mice survived up to the 70th day post infection, followed by infected subgroup treated with spiramycin; 95% of mice survived beyond the 55th day post infection, compared to 100% of mice in the RH infected control subgroup which died at the 7th day post infection (Fig. 2). Regarding *T. gondii* ME49 strain infected subgroups, 90% of mice infected and treated with SLCNs, survived beyond the 145th day post infection and 90% of infected mice subgroup treated with spiramycin survived up to the 120th day post infection, compared to 100% mortality rate in *T. gondii* ME49 strain infected control subgroup at the 60th day post infection (Fig. 3).

- Morphological study of *T. gondii* tachyzoites

Light microscopical examination of the tachyzoites in the peritoneal exudates of the different subgroups showed normal movement and shape in the infected control subgroup and infected subgroup received chitosan nanoparticles. While, tachyzoites in subgroup which were infected and treated with spiramycin, and infected subgroup treated with SLCNs, showed sluggish movement with deformed crescent shape (Figs. 4, 5, 6, 7, 8, 9, 10).

- Parasite count

There was a significant reduction in parasite count in the infected subgroup treated with spiramycin and the infected subgroup treated with SLCNs as compared to other subgroups with more reduction in the mean parasitic count in the subgroup received SLCNs in comparison to the others (Tables 1, 2).

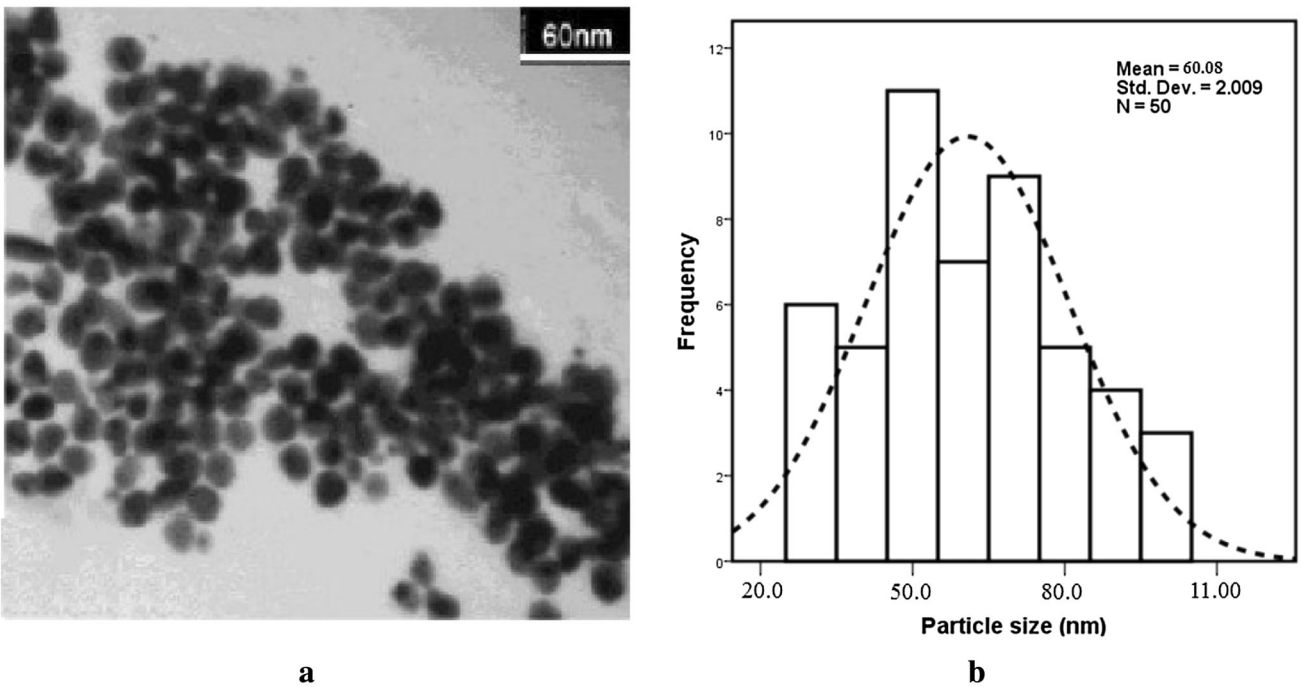

Fig. 1 SEM of spiramycin-loaded chitosan nanoparticles (SLCNs) showing regular, rounded shape with a smooth surface. Their mean size was 60.08 ± 2.009 nm

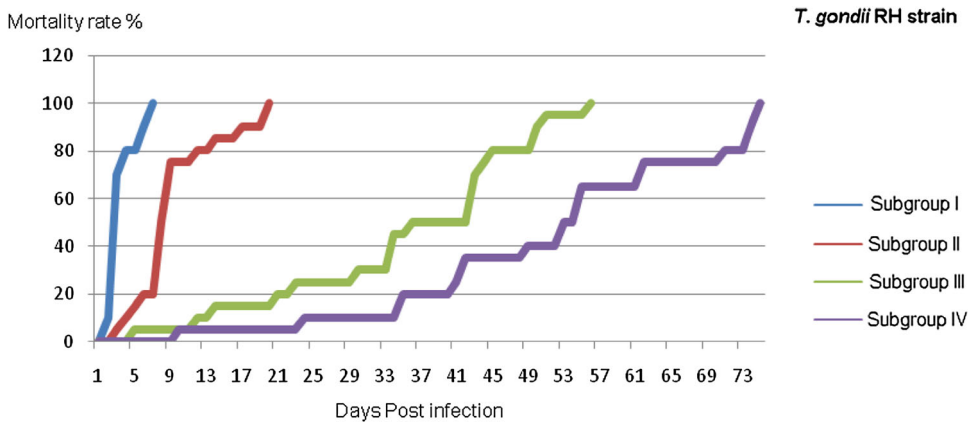

Fig. 2 The mortality rate of *T. gondii* RH infected subgroups; GI: RH infected control, GII: infected and received chitosan nanoparticles, GIII: infected and treated with spiamycin, GIV: infected and treated with SLCNs

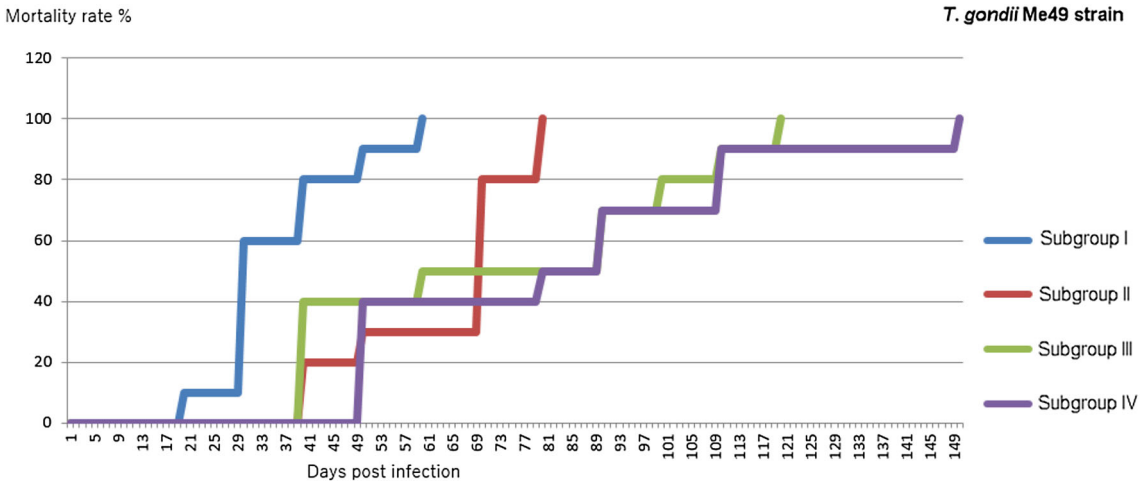

Fig. 3 The mortality rate of *T. gondii* Me49 strain infected subgroups; GI: Me49 infected control, GII: infected and received chitosan nanoparticles, GIII: infected and treated with Spiamycin, GIV: infected and treated with SLCNs

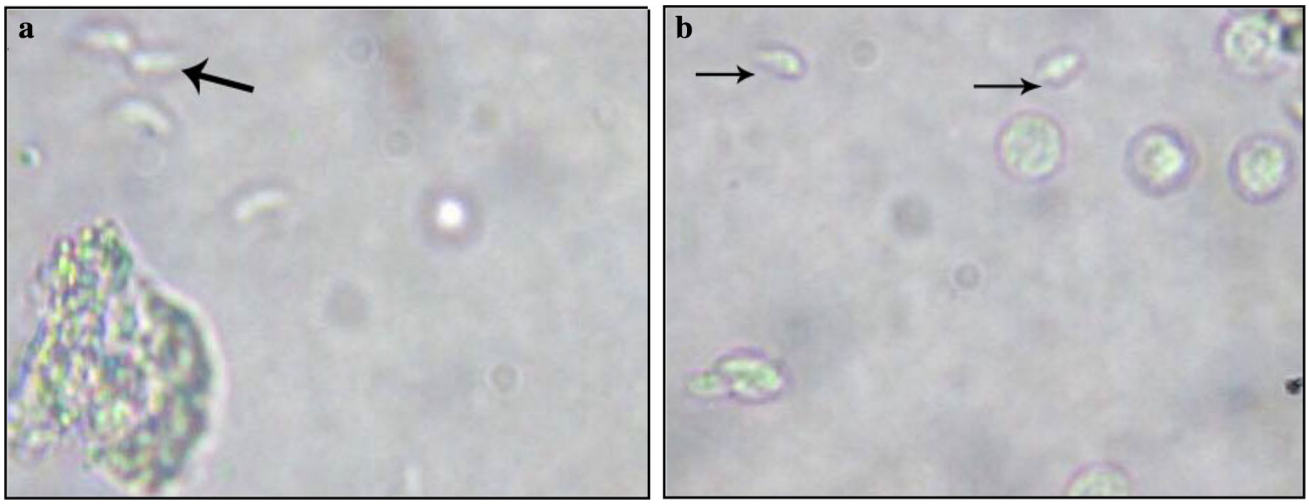

Fig. 4 LM examination of the tachyzoites in the peritoneal exudates of Rh strain infected mice. **a** Infected control subgroup showing the tachyzoites with a normal movement and shape, **b** infected subgroup treated with SLCNs showing tachyzoites with sluggish movement and deformed crescent shape

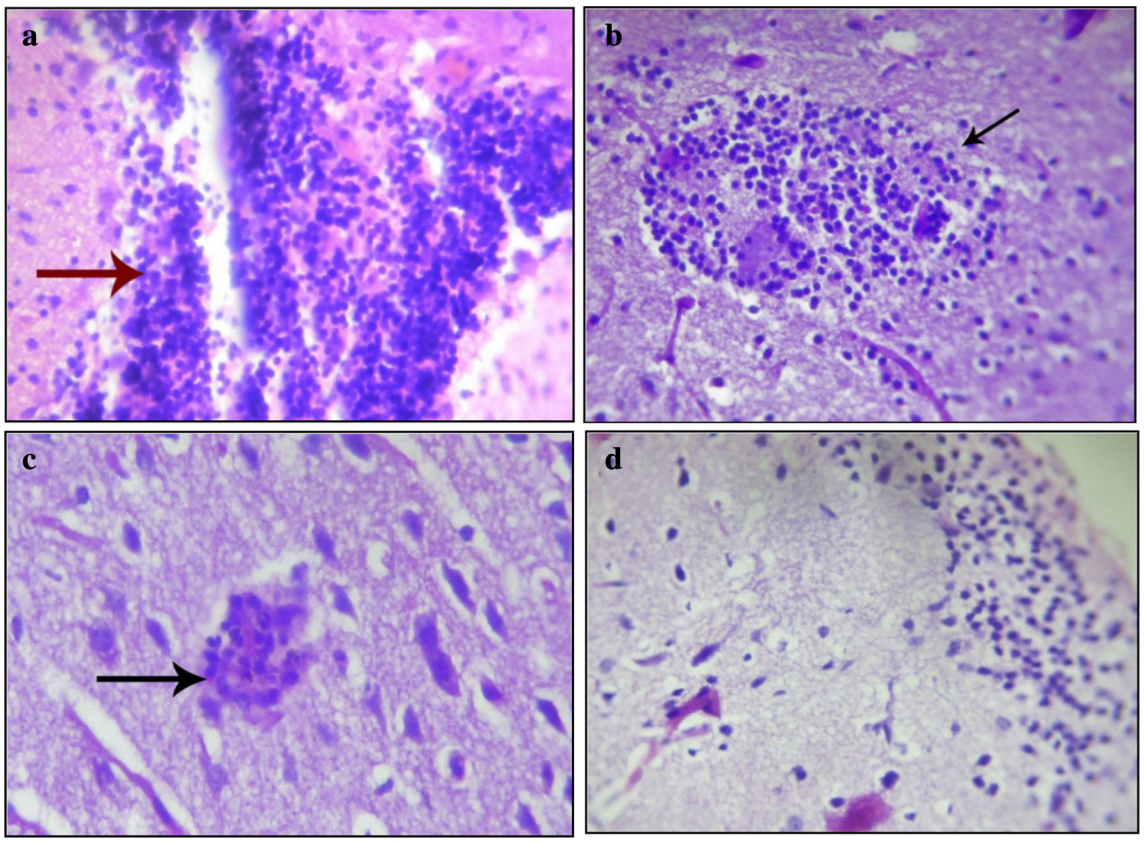

Fig. 5 Brain section of mice infected by *Toxoplasma* Rh strain. **a**, **b** Infected untreated control subgroup showing extensive perivascular inflammatory cellular infiltrates (H&E × 400). **c** Sections in the brain of spiramycin treated mice showing damaged pseudocyst (black arrow) with mild lymphocytic infiltrates and (H&E × 400). **d** Brain section of the mice subgroup infected and SLCNs treated revealing mild increase in the brain cellularity without lymphocytic infiltration (H&E × 400)

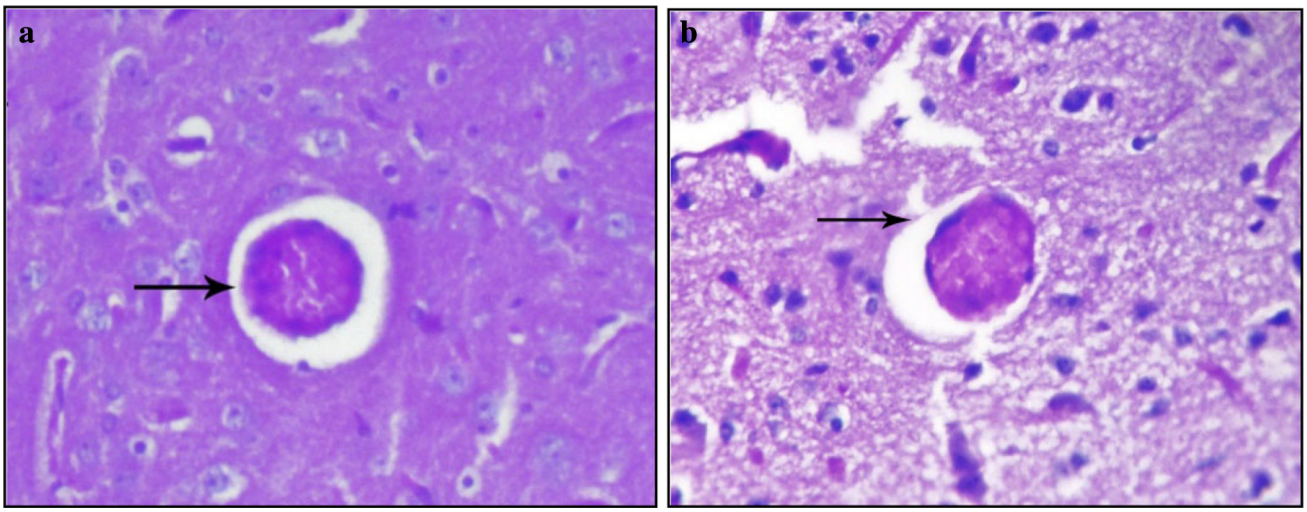

Fig. 6 Sections in the brain of *Toxoplasma* Me49 strain infected mice. **a** Brain section of spiramycin treated mice showing few number of *Toxoplasma* cysts with mild inflammatory cellular infiltrate (PAS × 400). **b** Brain section of mice infected and treated with SLCNs showing fewnumber of brain cysts without oedematous changes and a mild inflammatory cellular infiltrate (PAS × 400)

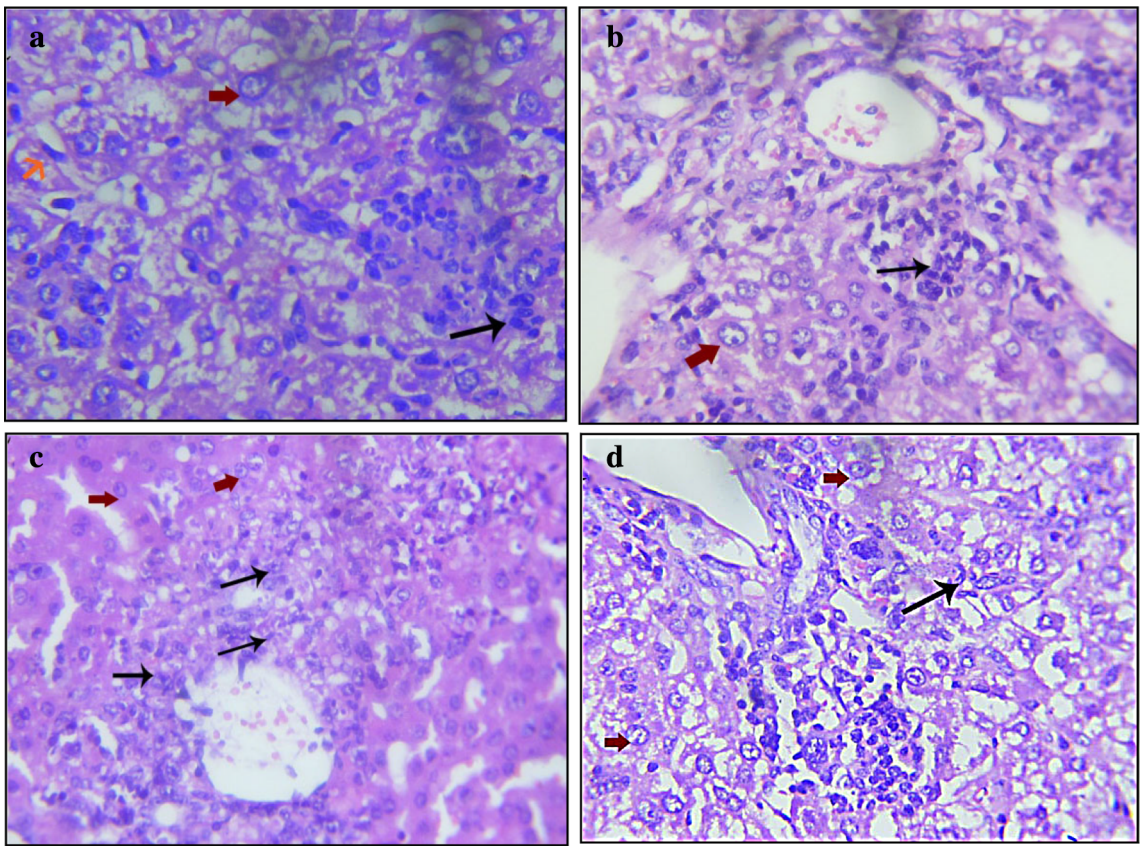

Fig. 7 Liver section of *Toxoplasma* Rh strain infected mice subgroups **a** infected untreated control subgroup showing disturbed architecture, extracellular tachyzoite collections (black arrow), Kupffer cells hyperplasia (orange arrows), hepatocyte diffuse ballooning with focal fatty degeneration (red thick arrow) (H&E × 400). **b** Sections in the liver of the mice subgroup given chitosan nanoparticles showed moderate portal tracts infiltration with chronic inflammatory cells in addition toextracellular tachyzoite collections (black arrow) and hepatocytes ballooning with fatty degeneration (red thick arrow) (H&E × 400). **c** Liver section of spiramycin treated mice revealing moderate cellular infilteration in the portal tract with few extracellular tachyzoite collections (black arrows) reduced inflammatory reaction (H&E × 400). **d** Sections in the liver of the mice subgroup infected and SLCNs treated showing mild degenerative changes of hepatocytes (red thick arrow) with few scattered extracellular parasites (black arrow) (H&E × 400) (colour figure online)

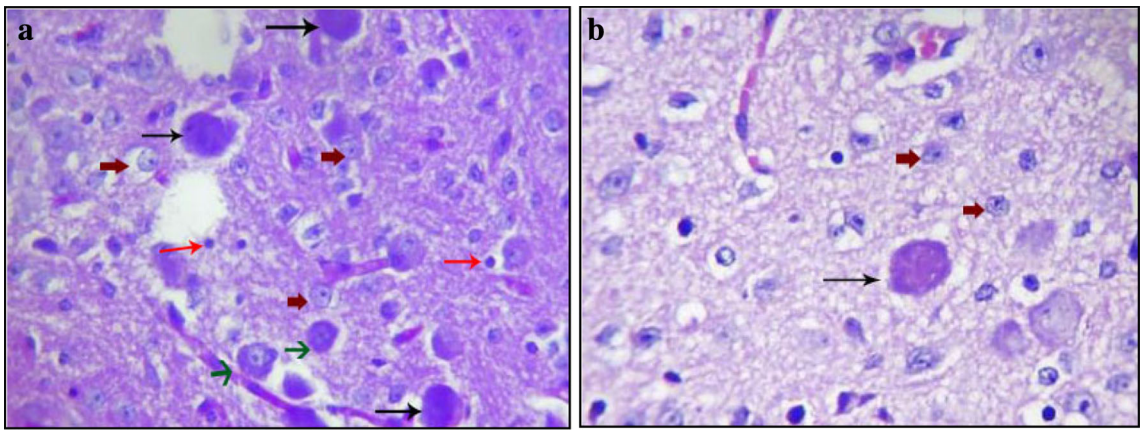

Fig. 8 Liver section of *Toxoplasma* Me49 strain infected mice. **a** Infected untreated control subgroup showing multiple *Toxoplasma* cysts (black arrows) with multiple inflammatory cells; lymphocytes (red arrows), histocytes (green arrows), mild fatty degeneration of hepatocytes (red thick arrows) (PAS × 400). **b** Liver section in infected mice treated with SLCNs, showing a single cyst (black arrow) with mild inflammatory reaction and mild hepatocyte degeneration (red thick arrow) (PAS × 400) (colour figure online)

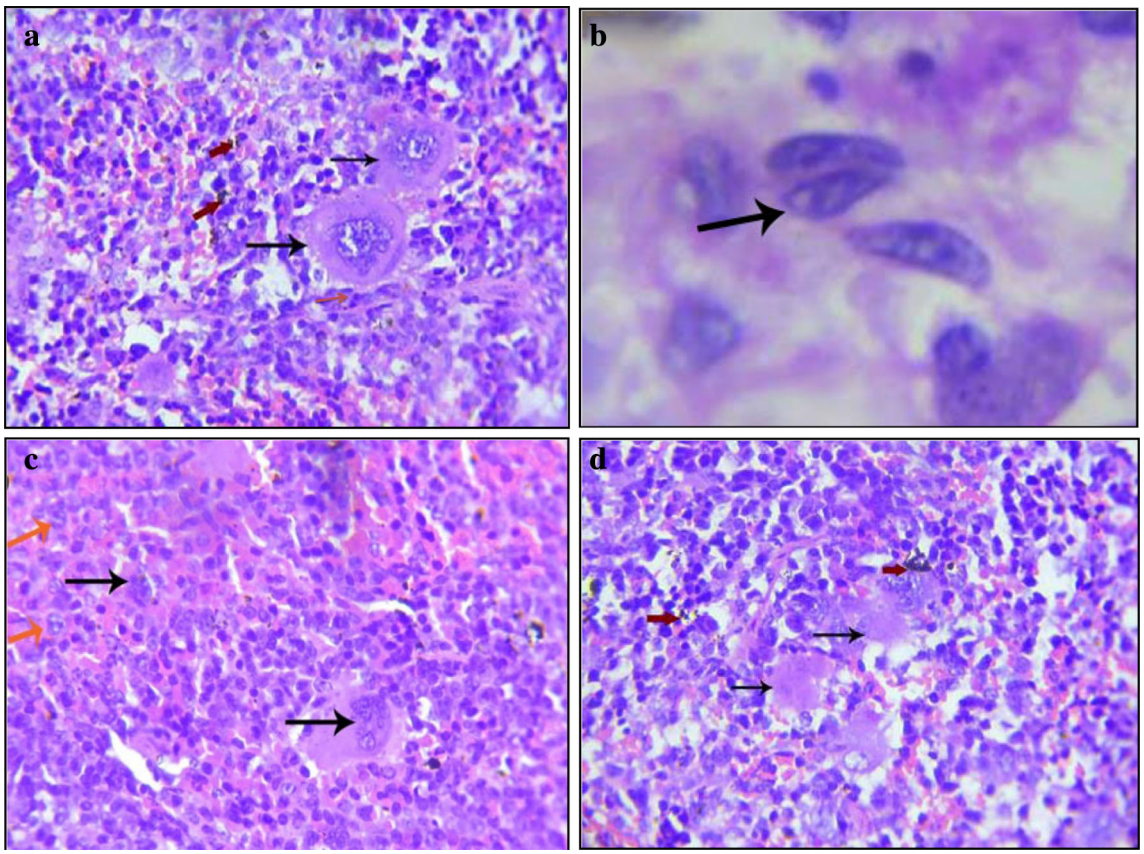

Fig. 9 Spleen section of *Toxoplasma* Rh strain infected mice subgroups. **a** Infected untreated control subgroup showing hyperplastic lymphoid follicles with hemosideriosis (red arrows), *Toxoplasma* pseudocyst containing tachyzoites (black arrow) and extracellular trophozoite (pink arrow). **b** A magnified number of extracellular tachyzoite collections (H&E × 400). **c** Spleen sections of mice subgroup infected and treated with spiramycin, showed few intracellular tachyzoites (black arrows) in the red pulp with many multinucleated giant cells (orange arrows) (H&E × 400). **d** Mice subgroup infected and treated with SLCNs revealed few tachyzoites extracellularly and degenerated pseudocysts (black arrows) with hemosiderosis in red pulps (red arrows) (H&E × 400) (colour figure online)

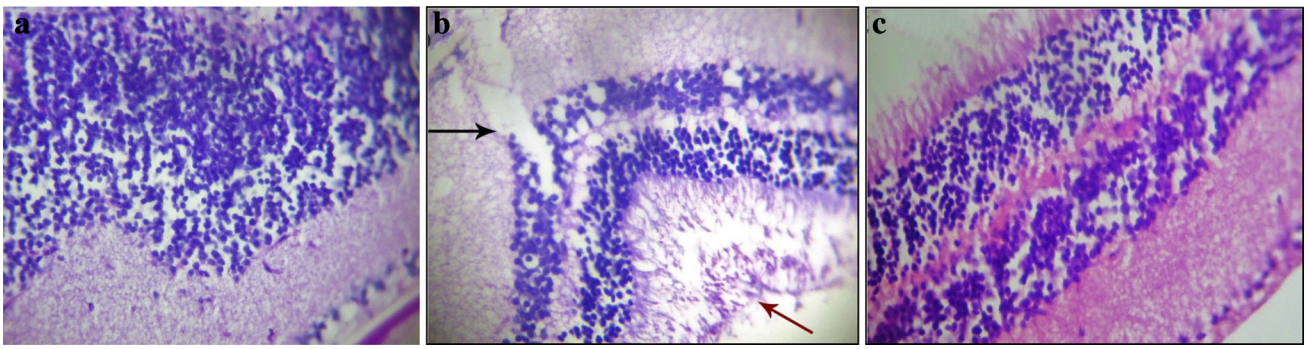

Fig. 10 Sections in the eye of *Toxoplasma* Me49 strain infected mice showing **a** infected untreated subgroup showing extensive inflammation (retinitis) composed of many lymphocytes and few macrophages affecting mainly the deep layers of the retina (PAS × 400) and **b** necrotizing retino-choroiditis "with extensive necrosis & disfigurement of retina & choroid" (PAS × 400). **c** Sections in the eye of SLCNs treated mice showing nearly normal structure

Table 1 The parasite count and the percentage reduction in the organs of RH infected mice

	Brain	Liver	Spleen
Subgroup I	1.09 ± 1.19	8.23 ± 2.10	3.51 ± 1.12
Subgroup II	1.02 ± 0.10[c,d]	6.26 ± 0.34[c,d]	2.89 ± 0.13[c,d]
% R1	6.42	23.94	17.66
Subgroup III	0.19 ± 0.33[a,b]	0.87 ± 0.11[a,b]	0.19 ± 0.19[a]
% R2	82.57	89.4	94.59
Subgroup IV	0.05 ± 0.11[a,b,c]	0.31 ± 0.34[a,b]	0.05 ± 0.10[a,b]
% R3	95.41	96.2	98.58
F	567.502	73.128	68.215
p	< 0.001	< 0.001	< 0.001

GI: RH infected control subgroup, GII: infected subgroup received chitosan nanoparticles, GIII: infected subgroup treated with spiamycin, GIV: infected subgroup treated with SLCNs, % R1 percentage of reduction in infected subgroup taken chitosan nanoparticles, % R2 percentage of reduction in infected subgroup treated with spiamycin, R3percentage of reduction in infected subgroup treated with SLCNs

F: F test (ANOVA)

$p \leq 0.05$(statistically significant)

[a]Significant with subgroup I

[b]Significant with subgroup II

[c]Significant with subgroup III

[d]Significant with subgroup IV

Table 2 The parasite count and the percentage reduction in the organs of Me49 infected mice

	Brain	Liver
Subgroup I	31.02 ± 2.52	6.11 ± 1.15
Subgroup II	9.0 ± 1.91[a,c,d]	5.14 ± 2.01[c,d]
% R1	70.99	15.88
Subgroup III	4.0 ± 2.12[a,b,d]	0.15 ± 1.4[a,b]
% R2	87.1	97.55
Subgroup IV	1.60 ± 0.18[a,b,c]	0.1 ± 1.21[a,b]
% R3	94.84	98.36
F	412.231	98.45
p	< 0.001	< 0.001

GI: Me49 infected control subgroup, GII: infected and received chitosan nanoparticles, GIII: infected and treated with spiramycin, GIV: infected and treated with SLCNs, % R1 percentage of reduction in infected subgroup taken chitosan nanoparticles, % R2 percentage of reduction in infected subgroup treated with spiamycin, R3percentage of reduction in infected subgroup treated with SLCNs

F: F test (ANOVA)

$p \leq 0.05$, statistically significant

[a]Significant with subgroup I

[b]Significant with subgroup II

[c]Significant with subgroup III

[d]Significant with subgroup IV

Histopathological study

- Brain

Brain sections of *Toxoplasma* RH strain infected untreated mice showed heavy perivascular inflammatory cellular infiltrates. Brain sections of spiramycin treated subgroup showed increased cellularity with mild lymphocytic infiltration and edematous changes, while brain sections of mice infected and treated with SLCNs showed mild increase in the brain cellularity without lymphocytic infiltration. Regarding *Toxoplasma* ME49 strain infected subgroups, brain sections of infected untreated mice showed *Toxoplasma* cysts enclosed with chronic inflammatory cells. Brain sections of spiramycin treated subgroup

showed edematous changes in the brain, few *Toxoplasma* cysts without inflammatory cellular infiltration and mild increase in the cellularity of the brain. As regard mice infected and treated with SLCNs, brain sections showed fewer number of brain cysts without edematous changes.

- Liver

Sections from the liver of the virulent RH strain infected control subgroup showed disturbance in the liver architecture and variable hepatocyte diffuse ballooning and focal fatty degenerative changes. Liver lobules revealed moderate inflammatory cellular infiltration and its sinusoids showed dilatation and infiltration with inflammatory cells with Kupffer cells hyperplasia. Liver sections of infected mice subgroup received chitosan nanoparticles, exhibited similar changes to the infected subgroup with mild hepatic inflammation and necrosis, moderate chronic inflammatory cellular infiltration in the portal tracts with dilated and congested vascular spaces. Regarding spiramycin treated subgroup, liver sections showed an obvious reduction of the inflammatory response with mild hepatocytes inflammation and necrosis and few tachyzoites. Regarding infected subgroup treated with SLCNs, there were a marked reduction in the lobular and portal tract inflammatory reaction and a decrease in the inflammatory cellular infiltration and in the number of tachyzoites.

Sections in the liver of *Toxoplasma* ME49 strain infected mice showed multiple *Toxoplasma* cysts in infected untreated subgroup with multiple inflammatory cells; lymphocytes, histocytes, mild fatty degeneration of hepatocytes. Liver sections in infected SLCNs treated subgroup showed few cysts with mild inflammatory reaction and mild hepatocyte degeneration.

- Spleen

Examination of the spleen of the RH strain infected mice showed hyperplastic lymphoid follicles and the sinusoids appeared dilated and congested with multinucleated giant. *Toxoplasma* pseudocysts were seen containing tachyzoites with marked congestion of the splenic red pulp with engorgement of the sinusoidal with macrophages containing tachyzoites. Some tachyzoite collections were seen extracellular within the red pulp, while the follicles of the white pulp showed hyperplasia.

Spleen sections of mice subgroup infected and treated with spiramycin, revealed few intracellular tachyzoites in the red pulp with many multinucleated giant cells. Mice subgroup infected and treated with SLCNs revealed mild white pulp follicular hyperplasia, the red pulp appeared congested with minimal sinusoidal histiocytosis and few tachyzoites inside and outside the cells.

- Eye

Sections in the eye of mice infected by *Toxoplasma* ME49 strain showed an area of extensive inflammation (retinitis) composed of many lymphocytes and few macrophages affecting mainly the deep layers of the retina. Moreover, necrotizing retino-choroiditis "with extensive necrosis and disfigurement of retina and choroid" was observed. Sections in the eye of SLCNs treated mice showed nearly normal structure.

Discussion

Chitosan is a natural polymer used in nanomedicines, as it has attractive characteristics for drug delivery and its formulated nanoparticulate form proved to be effective. Its cationic character and its solubility in aqueous medium have been reported as important properties for the success of this polysaccharide (Janes et al. 2001; Grenha et al. 2010). However, its ability to adhere to mucosal surfaces considered as the most attractive property (Blau et al. 2000; das Neves et al. 2011), leading to prolongation of its presence at drug absorption sites and increasing the drug permeation (Andrade et al. 2011). Capacity of chitosan to augment permeation of macromolecules epithelial through transient opening of epithelial tight junctions has been demonstrated. The polymer characterized by two mandatory requisites for drug delivery applications which are its biocompatibility and low toxicity (Andrade et al. 2011). Noticeably, the nanoparticulate form of chitosan has been proved to be more efficient for enhancing drug uptake when compared to solution form (Bowman and Leong 2006).

Many studies used nanoparticles as vehicles to deliver drugs for improvement of their therapeutic efficacy (Jiang et al. 2013; El-Zawawy et al. 2015; El-Temsahy et al. 2016).

Our study assessed the spiramycin-loaded chitosan nanoparticles (SLCNs) in the treatment of both *T. gondii* RH acute and ME49 chronic toxoplasmosis. It was noticed that SLCNs significantly decreased the mortality rate of mice infected by both strains compared to 100% mortality of mice in the infected control which died at the (7th day and 60th day post infection) in RH strain and ME49 strain respectively. This agreed with El-Temsahy et al. (2016) who noticed increasing in the survival time of mice after using chitosan nanospheres encapsulated with *Toxoplasma* lysate vaccine in both acute and chronic toxoplasmosis.

Estimation of parasite count could discover the density of infection in various tissues (El-Temsahy et al. 2002). In our study, impression smears revealed highly significant decrease in the number of organisms in the groups treated

with SLCNs as compared to the other subgroups. Similar significant reduction was noticed in mice treated by silver nanoparticles alone or combined with chitosan nanoparticles (Gaafar et al. 2014) and mice receiving *Nigella sativa oil* treatment (Mady et al. 2016).

Results of the parasite count agreed with the results of light microscopy. Morphological examination of tachyzoites by light microscopy revealed deformity and immobilization of organisms in the peritoneal exudates from mice of spiramycin and SLCNs treated subgroups but these changes were more noticed in the organisms from mice of SLCNs treated subgroups. Similar results were detected by Gaafar et al. (2014), when they used silver nanoparticles alone or in combination with chitosan in the treatment of experimental toxoplasmosis, and they explained the abnormalities in the shape of the organisms as a result to the effect of the drugs on DNA synthesis of the parasite or folic acid cycle.

For histopathological evaluation in this study, we used two stains; H&E and PAS stains. Glycoproteins are the main component in the wall membrane of *T. gondii* cyst which is important to maintain the parasite structure and its nutrient needs (Zhang et al. 2001). The periodic acid-Schiff (PAS) stain is used for staining of glycoprotein-containing tissues from different organs (Yamabayashi 1987). So, the cyst wall is periodic acid-Schiff (PAS) positive, whereas tachyzoites aren't (Boothroyd et al. 1997), which was apparent in our study.

Histopathological examination of the brain tissues in this work showed a moderate reduction in the pathological changes in the RH strain infected mice treated with spiramycin. While SLCNs caused a marked reduction as compared to infected control subgroup that showed extensive perivascular inflammatory cellular infiltration. These results agree with Mady et al. (2016) and Chen et al. (2013) who found that *T. gondii* infection stimulates a strong cellular immune response. Regarding *Toxoplasma* ME49 strain infected subgroups, brain sections of infected untreated mice revealed *Toxoplasma* cysts enclosed with chronic inflammatory cells. The same observations were reported by McLeod et al. (1988) and El-Temsahy et al. (2016).

Regarding histopathological examination of other organs, similar results were obtained, so we can conclude that loading of spiramycin on chitosan nanoparticles increases its approved potent therapeutic effect against experimental acute and chronic toxoplasmosis.

Acknowledgements We would like to thank Professor Iman F. Abou-El-Naga, professor and head of Medical Parasitology Department, Faculty of Medicine, Alexandria University, for providing the *Toxoplasma* strains. Special thanks to Dr. Eman H. Abdel-Bary, assistant professor of pathology, Zagazig University, for her assistance in pathological study.

Compliance with ethical standards

Conflict of interest Authors declare that there is no conflict of interest regarding the publication of this paper.

References

Ali M, Afzal M, Verma M, Misra-Bhattacharya S, Ahmad FJ, Dinda AK (2013) Improved antifilarial activity of ivermectin in chitosan–alginate nanoparticles against human lymphatic filarial parasite, *Brugia malayi*. Parasitol Res 112(8):2933–2943

Andrade F, Antunes F, Nascimento AV, da Silva SB, das Neves SB, Ferreira D, Sarmento B (2011) Chitosan formulations as carriers for therapeutic proteins. Curr Drug Discov Technol 8:157–172

Araujo FG, Phillippe P, Teri L, Remington SJ (1992) Activity of clarithromycin alone or in combination with other drugs for treatment of murine toxoplasmosis. Antimicrob Agent Chemother 36(11):2454–2457

Barakat AMA (2007) Some diagnostic studies on male New Zealand rabbit experimentally infected with *Toxoplasma gondii* strain. Glob Vet 1(1):17–23

Blau S, Jubeh TT, Haupt SM, Rubinstein A (2000) Drug targeting by surface cationization. Crit Rev Ther Drug Carr Syst 17:425–465

Boothroyd JC, Black M, Bonnefoy S, Hehl A, Knoll LJ, Manger ID, Ortega-Barria E, Tomavo S (1997) Genetic and biochemical analysis of development in *Toxoplasma gondii*. Philos Trans R Soc Lond B Biol Sci 352:1347–1354

Bowman K, Leong KW (2006) Chitosan nanoparticles for oral drug and gene delivery. Int J Nanomed 1:117–128

Briones E, Colino CI, Lanao JM (2008) Delivery systems to increase the selectivity of antibiotics in phagocytic cells. J Control Release 125(3):210–227

Bunetel L, Guerin J, Agnani G, Piel S, Pinsard H, Corbel JC, Bonnaure-Mallet M (2001) In vitro study of the effect of titanium on *Porphyromonas gingivalis* in the presence of metronidazole and spiramycin. Biomaterials 22:3067–3072

Chan YH (2003) Biostatistics 102: quantitative data—parametric & non-parametric tests. Singap Med J 44(8):391–396

Chan J, Luft BJ (1986) Activity of roxithromycin (RU 28965), macrolide, against *Toxoplasma gondii* infections in mice. Antimicrob Agents Chemother 30:323–324

Chan JM, Valencia PM, Zhang L, Langer R, Farokhzad OC (2010) Polymeric nanoparticles for drug delivery. Methods Mol Biol 624:163–175

Chen J, Huang SY, Zhou DH, Li ZY, Petersen E, Song HQ, Zhu XQ (2013) DNA immunization with eukaryotic initiation factor-2a of *Toxoplasma gondii* induces protective immunity against acute and chronic toxoplasmosis in mice. Vaccine 31(52):6225–6231

Choi WS, Kim HI, Kwak SS, Chung HY, Chung HY, Yamamoto K, Oguchi T, Tozuka Y, Yonemochi E, Terada K (2004) Amorphous ultrafine particle preparation for improvement of bioavailability of insoluble drugs: grinding characteristics of fine grinding mills. Int J Miner Process 74:S165–S172

Cottrellm AJ (1986) Acquired *Toxoplasma* encephalitis. Arch Dischild 61:84–85

Danesh-Bahreinni MA, Shokri J, Samiel A, Kamali-Sarvestani E, Barzegar-Jalali M, Mohmmadi-Samani S (2011) Nanovaccine for leishmaniasis; preparation of chitosan nanoparticles containing *Leishmania* superoxide dismutase and evaluation of its immunogenicity in BALB/C mice. Int J Nanomed 6:835–842

das Neves J, Bahia M, Amiji MM, Sarmento B (2011) Mucoadhesive nanomedicines: characterization and modulation of mucoadhesion at the nanoscale. Expert Opin Drug Deliv 8:1085–1104

Drury RAB, Wallington EA (1980) Carleton's histological technique, 5th edn. Oxford University Press, Oxford

Eissa MM, El-Azzouni MZ, Mady RF, Fathy FM, Baddour NM (2012) Initial characterization of an autoclaved *Toxoplasma* vaccine in mice. Exp Parasitol 131:310–316

El-Fakhry Y, Achbarou A, Desportes I, Mazier D (1998) Encephalitozoon intestinalis: humoral responses in interferon-γ receptor knockout mice infected with a *microsporidium* pathogenic in AIDS patients. Exp Parasitol 89:113–121

El-On J, Peiser J (2003) *Toxoplasma* and toxoplasmosis. Harefuah 142:48–55

El-Sayed NM, Aly EM (2014) *Toxoplasma gondii* infection can induce retinal DNA damage: an experimental study. Int J Ophthalmol 7(3):431–436

El-Temsahy MM, El-Kerdany ED, AbouShama LM (2002) Study of the role of antioxidant in experimental toxoplasmosis. J Med Res Inst 23(3):59–69

El-Temsahy MM, El Kerdany ED, Eissa MM, Shalaby TI, Talaat IM, Mogahed NM (2016) The effect of chitosan nanospheres on the immunogenicity of *Toxoplasma* lysate vaccine in mice. J Parasit Dis 40(3):611–626

El-Zawawy LA, El-Said D, Mossallam SF, Ramadan H, Younis SS (2015) Triclosan and triclosan-loaded liposomal nanoparticles in the treatment of acute experimental toxoplasmosis. Exp Parasitol 149:54–64

Engel G, Farid N, Faul M, Richardson L, Winneroski L (2000) Salt form selection and characterization of LY333531 mesylate monohydrate. Int J Pharm 198:239–247

Farinha A, Bica A, Tavares P (2000) Improved bioavailability of a micronized megestrol acetate tablet formulation in humans. Drug Dev Ind Pharm 26:567–570

Filice GA, Pomeroy C (1991) Effect of clindamycin on pneumonia from reactivation of *Toxoplasma gondii* infection in mice. Antimicrob Agents Chemother 35:780–782

Gaafar MR, Mady RF, Diab RG, Shalaby TI (2014) Chitosan and silver nanoparticles: promising anti-*toxoplasma* agents. Exp Parasitol 143:30–38

Giarcia LS, Bruckner DA (1977) Macroscopic and microscopic examination of fecal specimens. In: Giboda MN, Vokurkova P, Kopacek O (eds) Diagnostic medical parasitology, 3rd edn. ASM Press, Washington, pp 608–649

Grenha A, Al-Qadi S, Seijo B, Remuñán-Lopez C (2010) The potential of chitosan for pulmonary drug delivery. J Drug Deliv Sci Technol 20:33–43

Ing LY, Zin MN, Sarwaran A, Katas H (2012) Antifungal activity of chitosan nanoparticles and correlation with their physical properties. Int J Biomater 2012:632698

Israelski DM, Remington JS (1993) Toxoplasmosis in non-AIDS immunocompromised host. Curr Clin Top Infect Dis 13:322–356

Janes KA, Calvo P, Alonso MJ (2001) Polysaccharide colloidal particles as delivery systems for macromolecules. Adv Drug Deliv Rev 47:83–97

Jiang S, Hua E, Liang M, Liu B, Xie G (2013) A novel immunosensor for detecting *Toxoplasma gondii*-specific IgM based on goldmag nanoparticles and graphene sheets. Colloids Surf B Biointerfaces 101:481–486

Jongert E, Roberts CW, Gargano N, Forster-Waldi E, Petersen E (2009) Vaccines against *Toxoplasma gondii*: challenges and opportunities. Mem Inst Oswaldo Cruz Rio J 104(2):252–266

Kean T, Thanou M (2010) Biodegradation, biodistribution and toxicity of chitosan. Adv Drug Deliv Rev 62(1):3–11

Kernbaum S (1985) Susceptibility of *mycoplasmas* and *chlamydiae* to macrolides. J Antimicrob Chemother 16:199–200

Khalil NM, de Mattos AC, Carraro TC, Ludwig DB, Mainardes RM (2013) Nanotechnological strategies for the treatment of neglected diseases. Curr Pharm Des 19(41):7316–7329

Leslie E, Geoffrey J, James M (1991) Statistical analysis. In: Kirkpatrick LA, Feeney BC (eds) Interpretation and uses of medical statistics, 4th edn. Oxford Scientific Publications, Oxford, pp 411–416

Mady RF, El-Hadidy W, Elachy S (2016) Effect of *Nigella sativa* oil on experimental toxoplasmosis. Parasitol Res 115:379–390

Mcleod R, Frenkel JK, Estes RG, Mack DG, Eisenhauer PB, Gibori G (1988) Subcutaneous and intestinal vaccination with tachyzoites of *Toxoplasma gondii* and acquisition of immunity to per oral and congenital *Toxoplasma* challenge. J Immunol 140(5):1632–1637

Montoya JG, Remington JS (2008) Management of *Toxoplasma gondii* infection during pregnancy. Clin Infect Dis 47(4):554–566

Mourier P, Brun A (1997) Study of the metabolism of spiramycin in pig liver. J Chromatogr B 704:197–205

Paradkar A, Ambike A, Jadhav B, Mahadik K (2004) Characterization of curcumin-PVP solid dispersion obtained by spray drying. Int J Pharm 271:281–286

Penido MLO, Nelson DL, Vieira LQ, Coelho PMZ (1994) Schistosomal activity of alkyl aminooctanethiosulfuric acids. Mem Inst Oswaldo Cruz 89(4):595–602

Perng C, Kearney A, Palepu N, Smith B, Azzarano L (2003) Assessment of oral bioavailability enhancing approaches for SB-247083 using flow-through cell dissolution testing as one of the screens. Int J Pharm 250:147–156

Rubinstein E, Keller N (1998) Spiramycin renaissance. J Antimicrob Chemother 42:572–576

Said DE, ElSamad LM, Gohar YM (2012) Validity of silver, chitosan and curcumin nanoparticles as anti-*Giardia* agents. Parasitol Res 111:545–554

Salata OV (2004) Applications of nanoparticles in biology and medicine. J Nanobiotechnol 2(1):3

Saudi MNS, Gaafar MR, El-Azzouni MZ, Ibrahim MA, Eissa MM (2008) Synthesis and evaluation of some pyrimidine analogs against toxoplasmosis. Med Chem Res 17:541–563

Somnuk J, Anupap T, Virote B (2011) Preparation of chitosan nanoparticles for encapsulation and release of protein. Korean J Chem Eng 28(5):1247–1251

Thiptara A, Kongkaew W, Bilmad U, Bhumibhamon T, Anan S (2006) Toxoplasmosis in piglets. Ann NY Acad Sci 1081:336–338

Yamabayashi S (1987) Periodic acid—Schiff—Alcian Blue: a method for the differential staining of glycoproteins. Histochem J 19(10–11):565–571

Yamabayashi S, Tsukahara S (1987) Histochemical studies of the conjunctival goblet cells. I. (Alcian blue) AB (periodic acid-Schiff) PAS staining and PAS-AB staining. Ophthalmic Res 19:137–140

Zhang YW, Halonen SK, Ma YF, Wittner M, Weiss LM (2001) Initial characterization of CST1, a *Toxoplasma gondii* cyst wall glycoprotein. Infect Immun 69(1):501–507